



## Full Text View

[Volume 30, Issue 12 \(December 2000\)](#)

### Journal of Physical Oceanography

Article: pp. 3261–3269 | [Abstract](#) | [PDF \(882K\)](#)

## On the Variability of the Tropical Pacific Thermal Structure during the 1979–96 Period, as Deduced from XBT Sections

**Fabien Durand**

*LEGOS, Toulouse, France*

**Thierry Delcroix**

*Groupe ECOP, Centre IRD de Nouméa, Nouméa, New Caledonia*

(Manuscript received August 26, 1999, in final form July 5, 2000)

DOI: 10.1175/1520-0485(2000)030<3261:OTVOTT>2.0.CO;2

### ABSTRACT

The thermal structure variability of the tropical Pacific is investigated using an objective analysis of about 250 000 temperature profiles (mainly XBT) collected during the 1979–96 time period. Mean conditions and seasonal variability are briefly described to set the context, and temperature anomalies are constructed relative to a mean seasonal cycle to focus on the ENSO (El Niño–Southern Oscillation) timescale. Heat content anomalies (0–450 m) built up in the western equatorial basin prior to the 1982–83, 1986–87, and 1997–98 El Niño events but not clearly prior to the 1991–92, 1993, and 1994–95 events, which are thus found “atypical.” Low-frequency migration of temperature anomalies located at the mean thermocline depth is evidenced eastward in the equatorial band, as well as westward along a narrow zonal band located slightly north of the mean position of the intertropical convergence zone (say, 10°–20°N). This indicates that ENSO-related temperature anomalies in the subsurface ocean are present generally in the western equatorial Pacific about 1–2 years before the appearance of temperature anomalies in the eastern equatorial Pacific. Similarly, this indicates that subsurface temperature anomalies tend to be present in the eastern Pacific basin around 14°N about 1–2 years before the appearance of temperature anomalies in the western Pacific basin at the same latitude. The likely mechanisms responsible for these migrations and the possible link between the eastward and westward migration are discussed.

#### Table of Contents:

- [Introduction](#)
- [Data and processing](#)
- [Mean structure and seasonal](#)
- [Interannual variability](#)
- [REFERENCES](#)
- [FIGURES](#)

#### Options:

- [Create Reference](#)
- [Email this Article](#)
- [Add to MyArchive](#)
- [Search AMS Glossary](#)

#### Search CrossRef for:

- [Articles Citing This Article](#)

#### Search Google Scholar for:


- [Fabien Durand](#)
- [Thierry Delcroix](#)


Variability of the tropical Pacific thermal structure has been the subject of many investigations in the last two/three decades. In these investigations, one main source of information for the temperature field was, and still is, supplied by volunteer observing ships (VOS) providing expendable bathythermograph (XBT) data along selected merchant ship routes ([Donguy 1987](#)). The main items of knowledge gained from XBT data concern (i) the heat budget of the mixed layer ([Meyers et al. 1986](#)), (ii) the large-scale heat content and sea surface temperature (SST) changes ([White et al. 1985](#)), (iii) the geostrophic current systems ([Picaut and Tournier 1991](#)), and (iv) the ability of assimilated data into general circulation model for forecasting and/or hindcasting the El Niño–Southern Oscillation (ENSO) phenomenon ([Ji and Leetmaa 1997](#)).

To expand our knowledge of the variability of the tropical Pacific, the evolution of its thermal structure is investigated here over an 18-yr period extending from 1979 to 1996. This investigation is based on an objective analysis of a collection of temperature profiles derived chiefly from XBT, with additional mooring-derived measurements and occasional oceanographic cruises. The time period under study is of major interest as it covers numerous El Niño (1982–83, 1986–87, 1991–92, 1993, 1994–95) and La Niña (1988–89, 1995–96) events, known to be associated with extreme modification of the temperature field ([Hénin and Donguy 1980](#); [White et al. 1985](#); [Zhang and Levitus 1996](#); [Delcroix 1998](#)). The present study concentrates on the modification of temperature in a four-dimensional (4D) field (longitude, latitude, depth, and time), usefully complementing previous investigations which were restricted to shorter time series, and in most cases, simplified the 4D thermal field into a 3D field by looking at heat content and/or thermocline depth variability. In particular, this note focuses on the chronology of longitude–depths diagrams to further appraise the role of the ocean regarding the ENSO “memory” both for the equatorial band and possibly for an extra-equatorial region located slightly north of the mean position of the intertropical convergence zone (ITCZ).

The rest of the note is organized as follows: [section 2](#) presents the data and data processing; [section 3](#) describes the mean temperature structure and its seasonal variability, in order to set the context; and [section 4](#) focuses on ENSO-related heat content anomalies and concentrates on zonal displacements of temperature anomalies at depth.

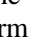
## 2. Data and processing

The 1979–84 XBT data originate from the compilation of [Picaut and Tournier \(1991\)](#), and the 1985–96 XBT data were obtained from the Subsurface Data Centre in Brest, France. The mooring-derived data were obtained from the TAO (Tropical Atmosphere Ocean) array consisting of nearly 70 moored buoys spanning the equatorial Pacific within 8°N–8°S ([Hayes et al. 1991](#); [McPhaden 1993](#)). Occasional cruises provided additional temperature profiles ([Delcroix et al. 1992](#)). All the temperature profiles (250 027) will be referred to simply as “XBT,” which represent about 80% of the profiles during 1979–96. The accuracy of temperature derived from XBT is of the order of 0.2°C. The spatial and temporal distribution of temperature profiles is shown in [Fig. 1](#) , illustrating the well-sampled areas related to the main shipping routes in the western, central, and eastern tropical Pacific, as well as to the TAO moorings in the equatorial band.

The XBT data were linearly interpolated in depth, every 10 m within 0–250 m, every 25 m within 250–500 m, and every 50 m down to 700 m. About 85% of the data reach 250 m, 80% reach 400 m and only 15% reach 700 m. Only the upper 450 m will be considered here. For each level, the data were objectively analyzed onto a regular 5° longitude × 1° latitude × 2 month grid. The decorrelation scales used in the objective analysis were 10° longitude, 2° latitude, and 2.5 months; these scales are close to the ones determined by [Meyers et al. \(1991\)](#) for the 18°N–18°S region (15° longitude, 3° latitude, and 2 months). On average, this results in about six samples per decorrelation scale at the surface. Our objective analysis routine provided estimates of errors normalized by the observed temperature variance in between 0 and 1. Based on comparisons with independent datasets (see details in [Durand 1998](#)), only temperature with errors less than 0.7 (i.e., 70% of the observed variance) are considered as representative. As expected, the representative temperature values are located chiefly along the main shipping tracks (shaded area in [Fig. 1b](#) .

A mean year, averaged over 2-month periods (Jan/Feb, . . . , Nov/Dec), was computed from the gridded temperature field, and temperature anomalies covering the 1979–96 period were then calculated relative to this mean year. Finally, a ¼–½–¼ filter was applied in space and time to reduce the small-scale variability. The 0–450 m heat content was defined as the average temperature of the upper 0–450 m.

## 3. Mean structure and seasonal variability

Maps of 1979–96 averaged SST, 0–450 m heat content and depth of the main thermocline estimated as the depth of the 20°C isotherm are shown in [Fig. 2](#) .

and stays rather flat west of this latter region, where the warm pool reaches about 75-m depth. The maximum variability around this mean structure stretches along the thermocline, with values over 2°C, reflecting vertical movements of isotherms occurring chiefly at seasonal and interannual timescales around the mean position of the thermocline.

The amplitude of the seasonal variability of temperature (not shown here) was defined as the standard deviation of the six 2-month averages of the mean year. At the surface, the maximum seasonal variability is found: (i) poleward of about 20° latitudes in relation with the seasonal variations of incoming solar radiation and (ii) in the equatorial band in the eastern half of the basin and along the south American coast, in relation with wind-driven equatorial and coastal upwelling. At 100-m depth, the maximum seasonal variability occurs within 4°N–12°N, in relation with vertical movements of the thermocline associated with seasonal changes in the wind stress curl related to the meridional shift of the ITCZ (Kessler 1990). At 200-m depth, two zonal bands of maximum seasonal variability exist around 5°S and 5°N in the western half of the basin, consistent with the signature of annual Rossby waves (Lukas and Firing 1985).

#### 4. Interannual variability

The interannual variability of the temperature field was documented by analyzing first the vertically averaged structures (i.e., the 0–450 m heat content anomalies), then the 4D distributions of temperature anomalies.

##### *a. Heat content anomalies*

The standard deviation of the 0–450 m heat content anomalies (not shown) presents a relative maximum in the eastern half of the equatorial basin and two relative maxima within both 5°–10° latitudes bands in the western half. These features are consistent with the schematic representation presented in Chao and Philander (1993). The eastern Pacific feature is reminiscent of interannual equatorial Kelvin waves, as the anomalies present a Gaussian shape trapped at the equator. The western Pacific feature is suggestive of remotely forced first-meridional-mode equatorial Rossby waves and/or of locally forced thermocline depth variations in response to Ekman pumping linked to interannual changes of the wind stress curl (see plate 6c in Delcroix 1998). A more detailed analysis (G. Alory 1999, personal communication) with 10-day resolution TOPEX/Poseidon sea level data covering the 1992–98 period, and a linear model output covering the 1961–98 period, suggest the dominance of remote forcing in these maxima, in agreement with McCreary (1978).

The succession of El Niño and La Niña events during the 1979–96 period shows up in the 5°N–5°S equatorial band (Fig. 4). In the eastern half of the basin, we observe nearly concurrent positive heat content and SST anomalies during the 1982–83, 1986–87, 1991–92, 1993, and 1994–95 El Niño, and negative heat content and SST anomalies during 1984 and the 1988–89 and 1995–96 La Niña. No significant SST anomalies are observed west of the date line. There, the heat content anomalies are out of phase with those located farther to the east. For example, maximum correlation coefficient between heat content anomalies at 0°–160°E and 0°–120°W is obtained when the 0°–160°E time series lags behind the one at 0°–120°W by 6–8 months.

An El Niño event is preceded generally by a buildup of heat content in the western Pacific warm pool, and its decline results in a discharge of the accumulated warm water to higher latitudes (Wyrtki 1985). A comparison between heat content anomalies at 0°–160°E (a point representative of the warm pool, see Figs. 2–4) and SST anomalies in the Niño-3 region (5°N–5°S, 150°W–90°W) indicates that this does not strictly apply for the 1979–96 period (Fig. 5). Indeed, while there was a slight buildup in 1979–81, 1985–86, and 1995–96 prior to the 1982–83, 1986–87, and 1997–98 El Niño, such a buildup did not occur before the 1991–92, 1993, and 1994–95 El Niño events that were, in fact, preceded by almost-zero or negative heat content anomalies (see also Kessler and McPhaden 1995). Moreover, a buildup appeared in the second half of 1988, during the mature phase of the 1988–89 La Niña. Hence, based on the apparent lack of buildup prior to the early 1990s events, it is tempting to claim that a buildup of heat content in the warm pool is neither sufficient nor necessary for an El Niño event to occur. To mitigate such a conclusion, it is worth noting that the appearance of a buildup is sensitive to the choice of a reference period. For example, if 1990–95 was chosen as a reference instead of 1979–96, then the 0-line in Fig. 5 would have been shifted by about –0.5°C and a build-up would show prior to the 1991–92 El Niño event. In other words, as discussed in Goddard and Graham (1997), if the mean state of the system changes, then the character of El Niño would be altered. Moreover, it should be kept in mind that the early 1990s may not be considered as El Niño (Trenberth and Hoar 1996; Goddard and Graham 1997).

##### *b. Subsurface temperature anomalies*

The longitude–time distribution of heat content anomalies in Fig. 4 indicates a tendency for eastward migration in the equatorial band, as already noted in previous studies (White et al. 1985). This migration may appear as a part of a continuous circuit running, schematically, from the west to the east along the equator and then from the east to the west along a narrow band centered around 14°N (Kessler 1990; Zhang and Levitus 1996; Delcroix 1998). Such a continuous circuit at the ENSO timescale was also documented with the 0–450 m heat content anomalies within our study (see Durand 1998).

To get a better insight of the nature of this circuit, as well as to determine the location of the anomalies at depths, the longitude–depth distributions of temperature anomalies were plotted for each time step covering the 1979–96 period, both along the equator and along 14°N. These plots (not all shown here) confirm the existence of such a circuit, especially prior to the 1990s and after 1995. This is exemplified in [Fig. 6](#) for the 1986–89 El Niño/La Niña period (see also [Goddard and Graham 1997](#); [Durand 1998](#)). On this figure, the temperature anomalies are centered at the mean thermocline depth: the warm anomalies migrate eastward along the equator from a depth of about 150 m in the west to 50 m in the east, and westward along 14°N from about 50 m in the east to 200 m in the west. The spatial distribution of temperature anomalies at the mean 20°C isotherm depth ([Fig. 7](#)) further evidences these zonal migrations, with the evidence of eastward migration in the equatorial band being stronger than that for westward migration within 10°–20°N.

In the equatorial band, a warm anomaly appeared in early 1986 in the west, reached the central basin by mid-1986, and the eastern basin in early 1987 ([Fig. 6](#)). Hence, the seeds of the 1986–87 El Niño were present at depths in the west about one year before its maximum surface oceanic manifestation in the east and in the atmosphere [see the Southern Oscillation index (SOI) in [Fig. 4](#)]. It is interesting to note that the warm anomalies observed in the eastern half of the basin by the end of 1986 were not balanced by cold anomalies in the western half, as would be expected if these anomalies only reflected an equatorial basin-scale zonal tilt of the thermocline. These zonally unbalanced anomalies also occurred by the end of 1987. This reinforces the idea that the warm pool filling-up and depletion not only result from zonal transport, but also from meridional transport, as demonstrated by [Gourdeau et al. \(2000\)](#) using a modeled velocity field corrected in assimilating TOPEX/Poseidon sea level data, and by [Meinen and McPhaden \(2000\)](#) using in situ temperature profiles.

The warm anomaly observed in the central-eastern equatorial Pacific in mid-1987 was reduced by the end of 1987. At that time, a warm anomaly could be observed at the mean thermocline depth within about 10°–20°N (and so at 14°N) in the eastern basin; it then reached the eastern-central basin in early 1988, the western-central basin in mid-1988, and the western basin by the end of 1988. The warm anomaly then appeared in the equatorial band in the west in the first half of 1989, closing the loop of the aforementioned continuous circuit.

A similar space–time evolution along both 10°–20°N and the equatorial band also applies for the cold anomalies in 1986–88, lagging about 1 year behind the warm anomalies in the equatorial band. This is partly visible in [Fig. 7](#) during 1986 within 10°–20°N, and then more clearly detectable from early 1987 to mid-1988 in the equatorial band. Hence, as for the 1986–87 El Niño, it seems that the seeds of the 1988–89 La Niña were present at depths in the western equatorial basin about 1–2 years before its surface oceanic manifestation in the eastern equatorial basin and in the atmosphere (see the SOI). Interestingly, the cold temperature anomalies reaching the eastern equatorial basin in mid-1988 was followed by cold anomalies within 10°–20°N east of 110°W by the end of 1988. However, these 10°–20°N anomalies did not move significantly westward in 1989. It is tempting to relate this lack of westward migrations to the absence of El Niño in 1990–91.

A time-lag correlation analysis was performed to further diagnose and summarize the low-frequency migration of the 1979–96 temperature anomalies at the mean thermocline depth. The longitude–depth distribution of the lag correlation is shown in [Fig. 8](#) along the equator (with a reference point at 160°E–120 m), and in [Fig. 9](#) along the 14°N latitude (with a reference point at 100°W–70 m). The locations of reference points, near the mean depth of the 20°C isotherm, were selected where we observe the maximum signal in temperature ([Figs. 2c](#) and [3c](#)). Computations of autocorrelation functions indicate that the decorrelation timescales for temperature range from 2 to 6 months depending on the location and depth. For 108 2-month averages (1979–96) this yields to a minimum of 18 (108/6) degrees of freedom, and only correlation coefficients in excess of 0.40 are significant at the 90% confidence level.

Both [Figs. 8](#) and [9](#) confirm the overall tendency for zonal migration of temperature anomalies during the whole 1979–96 period, as exemplified in [Figs. 6](#) and [7](#) for the 1986–89 period. The mean transit time along both the equator and 14°N is about 1.5 years (8–10 2-month periods) from one side of the Pacific basin to the other, which is about the mean ENSO return interval (3 years) for the eastward plus westward migrations.

In the equatorial band and at the surface, as demonstrated by [Picaut and Delcroix \(1995\)](#) for the 1986–89 period, and [Delcroix et al. \(2000\)](#) for the 1992–98 period, the ENSO-related zonal migration of the eastern edge of the warm pool chiefly reflects the signature of zonal current anomalies associated with a combination of first-baroclinic equatorial Kelvin and Rossby waves. These current anomalies average about  $25 \text{ cm s}^{-1}$  (1 order of magnitude smaller than the first baroclinic mode phase speed), that is about 120° longitude per 1.7 yr in agreement with the migration speed in [Fig. 8](#). The zonal migration of temperature anomalies at the thermocline depth likely results from the same cause in the western half of the basin, as the zonal velocity profile of the first baroclinic mode is almost uniform in the isothermal layer (see [Fig. 18](#) in [Delcroix et al. 1992](#)). Hence, we propose that the warm (cold) anomalies appear first in the west, in relation to the eastward (westward) advection of the eastern edge of the warm pool, and then in the east, in relation to downward (upward) motion of the thermocline induced by remotely forced downwelling (upwelling) Kelvin wave packets.

Along the 14°N latitude, based on [Fig. 9](#), the speed of the westward migration of temperature anomalies at the

thermocline depth is about  $20 \text{ cm s}^{-1}$  ( $100^\circ$  longitude in ten 2-month periods). This is consistent with the 1970–86 MBT and XBT data analysis of [Kessler \(1990\)](#), with the 1993–95 TOPEX/Poseidon sea level data analysis of [Chelton and Schlax \(1996\)](#), and with the simple long-wave model of [Meyers \(1979\)](#) and [Kessler \(1990\)](#). This westward migration has been, and still is, the subject of controversy regarding its possible role in establishing the ENSO timescale ([White et al. 1985](#); [Battisti 1989](#); [Kessler 1990](#)). The present 1979–96 observations shed some more light on the question, but they do not bring any definite answer as to whether or not the low-frequency eastward ( $y = 0$ ) and westward ( $y = 14^\circ\text{N}$ ) migration of subsurface temperature anomalies are linked. Clearly, it is desirable to completely understand the dynamic relationship between the apparently consistent eastward and westward migrations of ENSO signal, especially given its potential implication for ENSO prediction. The mechanisms responsible for the whole circuit are presently being investigated with high resolution TOPEX/Poseidon data and models with/without data assimilation.

### Acknowledgments

We express our gratitude to all scientists, officers, crewmembers, and data bank managers who participated in the huge collection of XBT data gathered at the Subsurface Data Centre in Brest, France. The TAO data were provided by M. McPhaden and collaborators from PMEL-NOAA in Seattle, WA. The objective analysis routine was given to us by P. de Mey from LEGOS in Toulouse, France. The crucial programming contribution of P. Rual in deriving the objectively analysed gridded temperature field was deeply appreciated. For one of us (FD), this note is part of a *Mémoire de Diplôme d'Etudes Approfondies* of the Paris VI University undertaken while visiting the IRD Centre in Noumea. Support from this institution has been greatly appreciated. Comments and constructive criticisms from two anonymous reviewers were very helpful.

---

### REFERENCES

- Battisti, D., 1989: On the role of off-equatorial oceanic Rossby waves during ENSO. *J. Phys. Oceanogr.*, **19**, 552–559. [Find this article online](#)
- Chao, Y., and S. G. Philander, 1993: On the structure of the Southern Oscillation. *J. Climate*, **6**, 450–469. [Find this article online](#)
- Chelton, D., and M. Schlax, 1996: Global observations of oceanic Rossby waves. *Science*, **272**, 234–238.
- Delcroix, T., 1998: Observed surface oceanic and atmospheric variability in the tropical Pacific at seasonal and ENSO time scales: a tentative overview. *J. Geophys. Res.*, **103**, 18 611–18 633.
- , G. Eldin, M. H. Radenac, J. Toole, and E. Firing, 1992: Variations of the western equatorial Pacific Ocean, 1986–1988. *J. Geophys. Res.*, **97**, 5423–5447.
- , B. Dewitte, Y. Dupenhoat, F. Masia, and J. Picaut, 2000: Equatorial waves and warm pool displacements during the 1992–98 ENSO events: Observations and modelling. *J. Geophys. Res.*, in press.
- Donguy, J. R., 1987: Recent advances in the knowledge of the climatic variations in the tropical Pacific Ocean. *Progress in Oceanography*, Vol. 19, Pergamon, 49–85.
- Durand, F., 1998: Variabilité de la structure thermique de l’océan Pacifique tropical au cours de la période 1979–1996. Mémoires de DEA, Sciences de la Mer, Océanographie Physique, 59 pp. [Available from Centre IRD de Nouméa, BP A5, 98848 Nouméa, New Caledonia.]
- Goddard, L., and N. Graham, 1997: El Niño in the 1990s. *J. Geophys. Res.*, **102**, 10 423–10 436.
- Gourdeau, L., J. Verron, T. Delcroix, A. Busalacchi, and R. Murtugudde, 2000: Assimilation of Topex/Poseidon altimetric data in a primitive equation model of the tropical Pacific Ocean, 1992–96. *J. Geophys. Res.*, **105**, 8473–8488.
- Hayes, S., L. Mangum, J. Picaut, A. Sumi, and K. Takeuchi, 1991: TOGA-TAO: A moored array for real time measurements in the tropical Pacific. *Bull. Amer. Meteor. Soc.*, **72**, 339–347. [Find this article online](#)
- Hénin, C., and J. R. Donguy, 1980: Heat content changes within the mixed layer of the equatorial Pacific Ocean. *J. Mar. Res.*, **38**, 767–780.
- Ji, M., and A. Leetmaa, 1997: Impact of data assimilation on ocean initialization and El Niño prediction. *Mon. Wea. Rev.*, **125**, 742–753. [Find this article online](#)
- Kessler, W., 1990: Observations of long Rossby waves in the northern tropical Pacific. *J. Geophys. Res.*, **95**, 5183–5217.
- , and M. McPhaden, 1995: The 1991–1993 El Niño in the central Pacific. *Deep-Sea Res.*, **42**, 295–333.

Lukas, R., and E. Firing, 1985: The annual Rossby wave in the central equatorial Pacific Ocean. *J. Phys. Oceanogr.*, **15**, 55–67. [Find this article online](#)

McCreary, J. P., 1978: Eastern tropical ocean response to changing wind system. *Review Papers of Equatorial Oceanography—FINE Workshop Proceedings*, Nova NYIT Press.

McPhaden, M., 1993: TOGA-TAO and the 1991–93 El Niño Southern Oscillation event. *Oceanography*, **6**, 36–44.

Meinen, C. S., and M. J. McPhaden, 2000: Interannual variability in warm water volume transports in the equatorial Pacific during 1993–99. *J. Phys. Oceanogr.*, in press.

Meyers, G., 1979: On the annual Rossby wave in the tropical north Pacific Ocean. *J. Phys. Oceanogr.*, **9**, 663–674. [Find this article online](#)

—, J. R. Donguy, and R. K. Reed, 1986: Evaporative cooling of the western equatorial Pacific Ocean by anomalous winds. *Nature*, **323**, 523–526.

—, H. Phillips, N. Smith, and J. Sprintall, 1991: Space and time scales for optimal interpolation of temperature—tropical Pacific Ocean. *Progress in Oceanography*, Vol. 28, Pergamon, 189–218.

Picaut, J., and R. Tournier, 1991: Monitoring the 1979–1985 equatorial Pacific current transports with expendable bathythermograph data. *J. Geophys. Res.*, **96**, 3263–3277.

—, and T. Delcroix, 1995: Equatorial wave sequence associated with warm pool displacement during the 1986–1989 El Niño and La Niña. *J. Geophys. Res.*, **100**, 398–408.

Trenberth, K., and T. Hoar, 1996: The 1990–1995 El Niño–Southern Oscillation event: Longest on record. *Geophys. Res. Lett.*, **23**, 57–60.

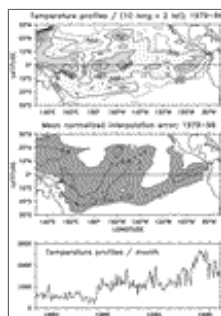
White, W., G. Meyers, J. R. Donguy, and S. Pazan, 1985: Short-term climatic variability in the thermal structure of the Pacific Ocean during 1979–82. *J. Phys. Oceanogr.*, **15**, 917–935. [Find this article online](#)

Wyrtki, K., 1974: Sea level and the seasonal fluctuations of the equatorial currents in the western Pacific Ocean. *J. Phys. Oceanogr.*, **4**, 91–103. [Find this article online](#)

—, 1985: Water displacements in the Pacific and the genesis of El Niño cycles. *J. Geophys. Res.*, **90**, 7129–7132.

Zhang, R. H., and S. Levitus, 1996: Structure and evolution of interannual variability of the tropical Pacific upper ocean temperature. *J. Geophys. Res.*, **101**, 20 501–20 524.

## Figures



[Click on thumbnail for full-sized image.](#)

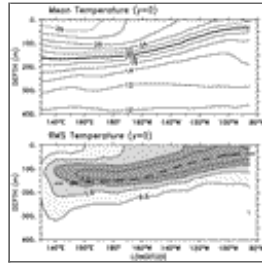
Fig. 1. (top) Number of temperature profiles (mostly XBT) in  $2^\circ$  lat  $\times$   $10^\circ$  long boxes collected in the tropical Pacific during 1979–96. The contour interval is 500, except for the dashed 250 isoline. (middle) Mean normalized interpolation error for the analysis of near-surface temperature. Contour intervals are drawn only for 0.4 and 0.7 isolines, and the area where the error is less than 0.7 is shaded. (bottom) Time series of the number of temperature profiles collected per month in the tropical Pacific





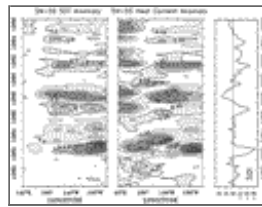
[Click on thumbnail for full-sized image.](#)

Fig. 2. Mean (top) sea surface temperature, (middle) 0–450 m heat content, and (bottom) depth of the 20°C isotherm during 1979–96. The contour interval is 1°C for the two upper panels and 20 m for the bottom panel



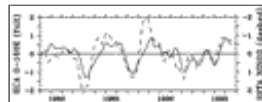
[Click on thumbnail for full-sized image.](#)

Fig. 3. Longitude–depth diagram of (top) 1979–96 mean temperature and (bottom) the associated standard deviation (rms) along the equator. The contour interval is 2°C in the top panel, except for the dashed 29°C isotherm, and it is 0.5°C in the bottom panel. The heavy dashed line in the bottom panel represents the mean position of the 20°C isotherm



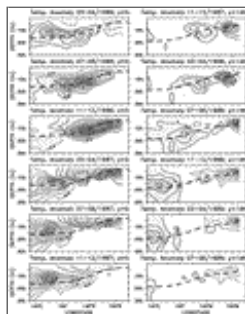
[Click on thumbnail for full-sized image.](#)

Fig. 4. Longitude–time diagram of 5°N–5°S averaged (left) SST anomalies and (middle) 0–450 m heat content anomalies. The contour interval is 0.5°C for the SST, 0.25°C for the heat content, and the 0-isolines are omitted. The right panel represents the Southern Oscillation index (SOI) filtered with a 3-month Hanning filter



[Click on thumbnail for full-sized image.](#)

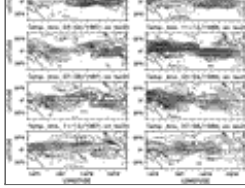
Fig. 5. Comparison between (full line, left vertical scale increasing upward) 0–450 m heat content anomalies at 0°–160°E and (dashed line, right vertical scale increasing downward) SST anomalies in the Niño-3 region defined within 5°N–5°S, 150°W–90°W. Units are degrees Celsius



[Click on thumbnail for full-sized image.](#)

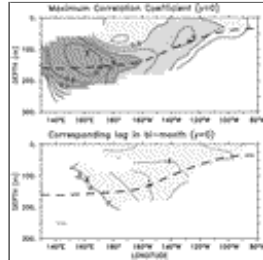
Fig. 6. Time sequences of bimonthly temperature anomalies along (left figures) the equator and (right figures) 14°N during the 1986–89 El Niño/La Niña event. The contour interval is 0.5°C, the 0-isolines are omitted in all figures. The heavy-dashed lines on each figures indicate the 1979–96 mean positions of the thermocline chosen as the 20°C isotherm (see Fig. 3c). Time increases downward on both panels and the Nov/Dec 1987 period appears both on the bottom-left and upper-right panels to ease interpretation. Values are not representative within 160°E and 180° on the right figures (normalized errors > 0.7):





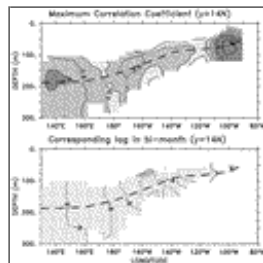
[Click on thumbnail for full-sized image.](#)

Fig. 7. Time sequences of bimonthly temperature anomalies at the mean 20°C isotherm depth ([Fig. 3c](#)). The contour interval is 0.5°C, the 0-isolines are omitted in all figures. Only values located where the mean normalized error ([Fig. 1b](#)) is less than 0.7 can be considered as representative



[Click on thumbnail for full-sized image.](#)

Fig. 8. Longitude–depth diagram along the equator of (top) maximum correlation coefficients at (bottom) given lag between time series of temperature anomalies and the reference time series located at 160°E, 120 m (× symbol). The lags are expressed in 2-month periods; a negative lag indicates that the time series lags behind the reference time series. Correlation (R) and lag are reported only when R is significant at the 90% confidence level



[Click on thumbnail for full-sized image.](#)

Fig. 9. Same as [Fig. 8](#) but along 14°N and with a reference point at 100°W, 70 m

Corresponding author address: Dr. Thierry Delcroix, IRD, ECOP Group, B.P. A5, 98848 Noumea, New Caledonia.

E-mail: [delcroix@noumea.ird.nc](mailto:delcroix@noumea.ird.nc)

[top](#) ▲



© 2008 American Meteorological Society [Privacy Policy and Disclaimer](#)  
 Headquarters: 45 Beacon Street Boston, MA 02108-3693  
 DC Office: 1120 G Street, NW, Suite 800 Washington DC, 20005-3826  
[amsinfo@ametsoc.org](mailto:amsinfo@ametsoc.org) Phone: 617-227-2425 Fax: 617-742-8718  
 Allen Press, Inc. assists in the online publication of AMS journals.